Journal of Chemical Health Risks 3(2): 15-26, 2013
ISSN:2251-6719

Electrospun Nanofibrous Membranes as Potential Adsorbents for Textile Dye Removal-A review

M. Hasanzadeh, B. Hadavi Moghadam*

Department of Textile Engineering, University of Guilan, Rasht, Iran

(Received: 30 March 2013 Accepted: 15 June 2013)

Abstract: Textile wastewaters due to the toxic effects of dyestuffs and other organic compounds and their stability toward light and oxidizing agents have led to an environmental problem. Several treatment methods for dye removal have been investigated. Membrane process is one of the simplest and most effective methods for dye removal from industrial wastewaters. Electrospun nanofibrous membranes have high specific surface area, high porosity, and small pore size. Therefore, they have been suggested as excellent candidates for many applications, especially in wastewater treatment. In this paper, we introduce the fundamental aspects of electrospun nanofibrous membranes and their properties, as well as highlight the enormous potential of nanofibrous membrane as adsorbents for textile dye removal. Finally, characteristic parameters for membrane performance are enumerated. Permeation flux, rejection, membrane porosity, permeability, molecular weight cut off, and decolorization are considered to be the most important ones.

Keywords: Nanofibrous membrane, Wastewater, Electrospinning, Dye removal, Efficiency

INTRODUCTION

Synthetic dyes have been widely used as colorants at different industries such as textile, food, paper, pharmaceutical, cosmetic, etc. The textile dyeing industry consumes large quantities of water and produces large volumes of wastewater from different steps in the dyeing and finishing, among other processes. Textile wastewaters present an environmental problem because of the non-biodegradable nature of dyes and their stability toward light and oxidizing agents. Moreover, some of the dyes and dyeing axillaries are toxic and contribute to the high biological oxygen demand (BOD) or chemical oxygen demand (COD) values of the effluents. Thus, the treatment of dye contaminated wastewater has become environmentally important because of increased awareness of environmental issues throughout the world [1-6].

Several treatment methods for dye removal have been investigated, including adsorption [7, 8], membrane process [9], electrochemical [10], coagulation-flocculation [11], biological [12,13], etc. Membrane process, including microfiltration, ultrafiltration, nanofiltration, and reverse osmosis, as a simple and effective method to remove a large number of dyeing auxiliaries and organic compounds has been widely studied (see Figure 1). These techniques are increasingly being used in the treatment of textile wastewater. Until now a number of studies deal with application of membrane filtration process in the treatment wastewater from the dyeing and finishing process.

Corresponding Author: M. Hasanzadeh, Department of Textile Engineering, University of Guilan, Rasht, Iran
E-mail: hasanzadeh_mahdi@yahoo.com

Membrane processes provide very interesting possibilities for the separation of dyeing auxiliaries that reduce coloration and BOD or COD of the wastewater [14, 15].

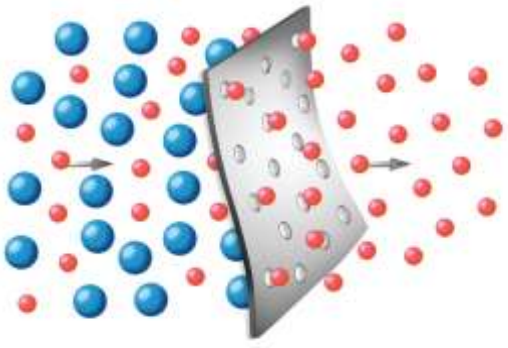

Figure 1. Schematic representation of membrane process.

NANOFIBROUS MEMBRANE

Nanofibrous membrane can be processed by a number of techniques such as drawing [16], template synthesis [17], phase separation [18], self-assembly [19], and electrospinning [20]. Among them electrospinning, which has an advantage with its comparative low cost and relatively high production rate, has attracted increasing attention during the last two decade. In this process, a strong electric field is applied between polymer solution contained in a syringe with a capillary tip and grounded collector. When the electric field overcomes the surface tension force, the charged polymer solution forms a liquid jet and travels towards collection plate. As the jet travels through the air, the solvent evaporates and dry fibers deposits on the surface of a collector [21-28]. Figure 2 shows a schematic illustration of electrospinning setup.

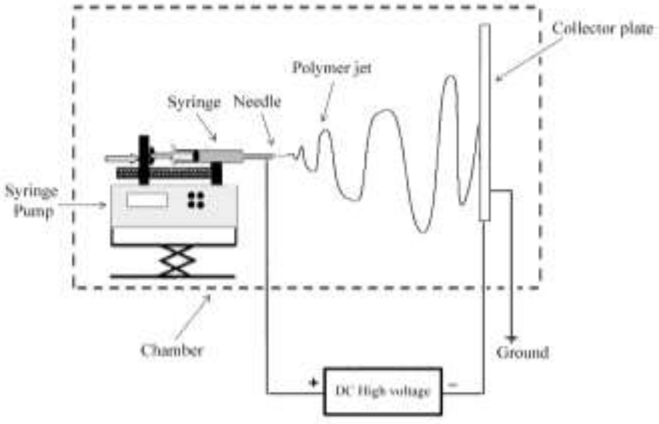

Figure 2. The schematic illustration of electrospinning setup.

The morphology and the structure of the electrospun nanofibrous membrane are dependent upon many parameters which are mainly divided into three categories: solution properties (the concentration, liquid viscosity, surface tension, and dielectric properties of the polymer solution), processing parameters (applied voltage, volume flow rate, tip to collector distance, and the strength of the applied electric field), and ambient conditions (temperature, atmospheric pressure, and humidity) [22-29]. Table 1 summarizes the effects of all the electrospinning parameters on the nanofibrous membrane morphology.

Table 1. Electrospinning process parameters and their effects on nanofiber morphology [24]

Electrospinning parameters		**Effect on nanofiber morphology**
Solution properties	Concentration	Increase in concentration leads to increase in fiber diameter.
	Viscosity	Increasing viscosity leads to thicker and beadless nanofibers. Too high viscosity causes generation of beads.
	Surface tension	No conclusive correlation has been established between the surface tension and the nanofiber morphology.
	Conductivity	Increase in conductivity leads to thinner nanofibers.
	Polymer molecular weight	Increase in polymer molecular weight leads to formation of a nanofiber with fewer beads.
	Solvent volatility	Higher volatility requires higher flow rate and leads to formation of a nanofiber with fewer beads.
	Dielectric constant	Sufficient dielectric constant of the solvent is needed for successful electrospinning.
Processing parameters	Applied voltage	Thinner fiber with higher applied voltage.
	Volume flow rate	Lower flow rate results in thinner nanofibers. Too high flow rate causes the generation of beads.
	Tip-to-collector distance	Minimum distance required to obtain dry nanofibers. Generation of beads when the distance is too small or too large.
	Collector geometry	Metal collectors are preferred. With conductive frame or rotating drum aligned nanofibers are obtained.
Ambient conditions	Temperature	Thinner nanofibers are obtained when the temperature is higher.
	Humidity	Lower humidity enables higher flow rate and the generation of beads is reduced.

Different types of nanofibrous membranes

The unique advantage of nanofibrous membranes is that they combine high specific surface area with a permeable and easily handled mat structure. By varying the electrospinning parameters, it is possible to get some variation in the morphology of the nanofibrous membrane. Several approaches to modifying the surface morphology of nanofibrous membrane have been discussed in a number of researches.

Porousnanofibers

There are many parameters that may contribute to the formation of pores on nanofibers during electrospinning such as humidity, type of polymer, solvent vapor pressure, electrospinning conditions, etc. Although no generally agreed set of definitions exists, porous materials can be classified in terms of their pore sizes into various categories including capillaries (>200 nm), macropores (50-200 nm), mesopores (2-50 nm) and micropores (0.5-2 nm) [30]. According to the literature, the mechanism that forms porous surface on polymer casting film is applicable to the phenomenon on electrospun nanofibers [30]. The rapid solvent evaporation and subsequent condensation of moisture into water particles result in the formation of nano- or micropores on the fiber surface (see Figure 3). When the environment humidity increases, the pore size becomes larger. However, this result was observed only when the solution used a highly volatile organic solvent, such as chloroform, tetrahydrofuran, and acetone.

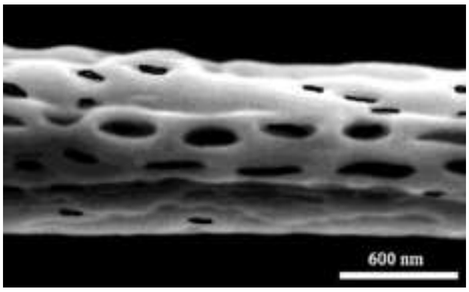

Figure 3. SEM micrograph of polycarbonate porous nanofibrous membrane [30].

Bicomponent nanofibers

Similar to conventional bicomponent fibers, a bicomponent nanofiber consists of two or more polymer components within the same filament, with each component existing separately. Typically, the bicomponent nanofibers can be classified into four main types: ‘core–sheath’, ‘side-by-side’, ‘pie-wedge’ and ‘islands in the sea’. Their cross-sectional morphologies are illustrated in Figure 4. Although the existing fiber-making technique is able to produce a bicomponent fiber of many cross-sectional structures, the production of bicomponent nanofibers has been limited to two basic types of cross-sectional structures, the ‘core–sheath’ and the ‘side-by-side’ [30].

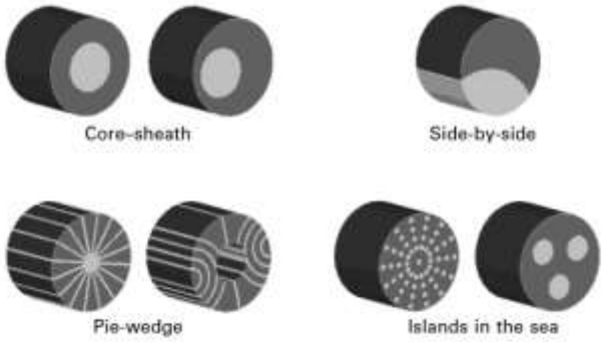

Figure 4. Cross-sectional morphologies of the bicomponent fibers [31].

These bicomponent nanofibers are electrospun via special spinnerets. Two polymer solutions flow within the spinneret as the sheath and core, or side-by-side, to the tip of the nozzle and then are subjected to a co-electrospinning process.

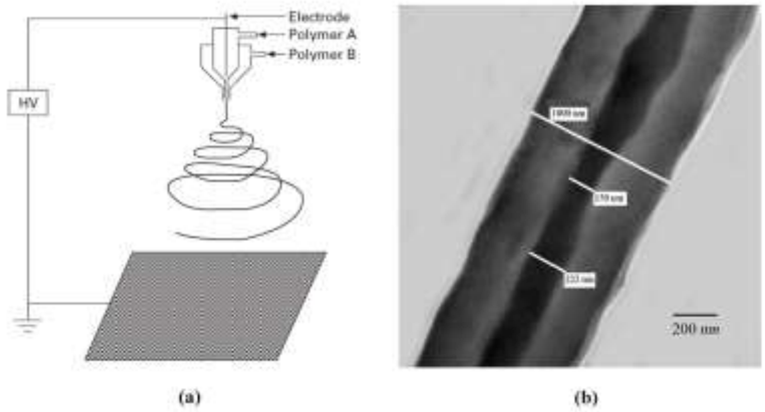

Figure 5. (a) Apparatus for electrospinning core–sheath nanofibers, (b) TEM micrograph of bicomponent nanofibers [31,32].

Hollow nanofibers

By employing the electrospinning process, chemical vapor deposition (CVD) method and direct co-axial spinning method, hollow nanofibers can be made. The CVD method is down as follows (see Figure 6). First, the template polymer nanofibers are electrospun before they are coated by sheath material by CVD. Hollow nanofibers are finally formed when the template is removed via annealing. To attain this, the template nanofiber should be stable during the coating but degradable or extractable without destroying the coating layer [33].

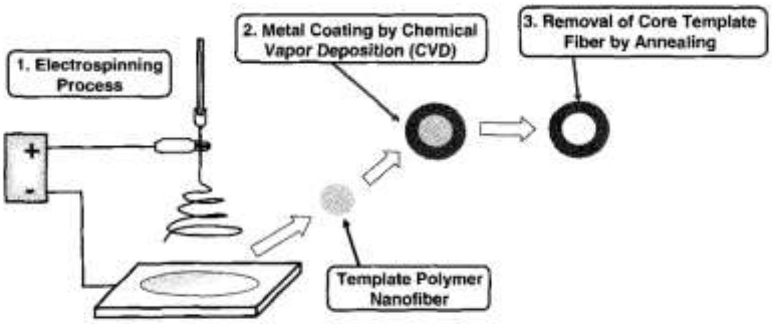

Figure 6. Hollow nanofibers made by chemical vapor deposition method [33].

Direct co-axial spinning method offers one-step processing of hollow nanofibers, including direct co-axial electrospinning process to create a core-sheath nanofiber and finally removing core material by chemical solvent or annealing.

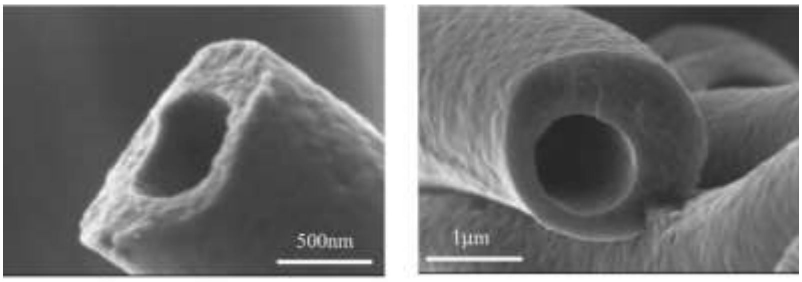

Figure 7. SEM micrograph of carbonized hollow nanofibers [34].

Composite nanofibers

Sometimes it is necessary to have more than one material in nanofibrous membrane to mimic the structural and mechanical properties of the membranes. Nanocomposite nanofibrous membrane (nanoscale fibers that include nanoparticulate fillers), present a more complex situation as nanofiber diameters allow only a very limited size range of candidate nanoparticles to be accommodated within the composite fiber. A range of different nanomaterials has been successfully electrospun in polymer solutions to yield composite nanofibrous membrane [30]. Figure 8 illustrates the SEM and TEM micrograph of SWNT/PAN nanofibrous membrane.

Incorporation of CNT into polymer matrix, due to the exceptional properties and large aspect ratio, has been proven to be a promising approach leading to structural materials and composites with excellent physical and mechanical properties such as tensile strength, tensile modulus, strain to failure, torsional modulus, compressive strength, glass transition temperature, solvent resistance, and reduced shrinkage. Electrospinning as an effective processing method to produce CNT-polymer nanofibrous membrane with the CNTs orienting to the axes of the as-spun nanofibers have attracted increasing attention during the last two decades (see Figure 9). However, particular attention needs to be paid to achieve a good dispersion of nanotubes in the spinning solution to maximize mechanical properties of the membranes [30].

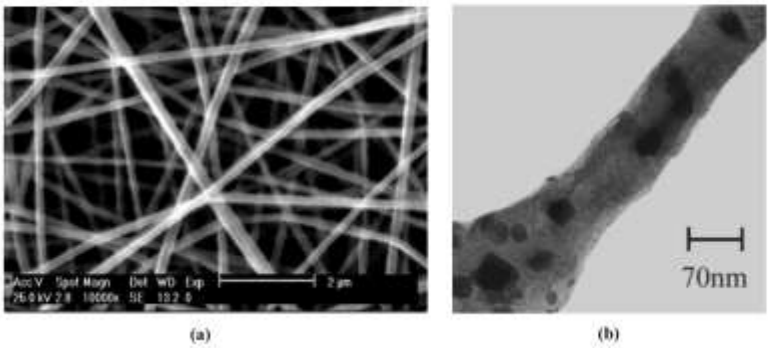

Figure 8. (a) SEM, and (b) TEM micrograph of PAN/SWNT composite nanofibers [35].

The exceptional structure of CNTs, their low density, their high aspect ratio, and outstanding mechanical and physical properties make them an ideal candidate for specific applications in which CNTs are used as reinforcements in composite membranes. There are several parameters affect the mechanical properties of composite membranes, including large aspect ratio of reinforcement, good dispersion, alignment and interfacial stress transfer [38-39].

It is well known that CNTs are insoluble in water or other solvents but can be suspended or dispersed in liquids. Optimal reinforcement of the composite nanofibrous membrane depends on the extent of the dispersion of CNTs in the spinning solution. Many different approaches have been used by researchers in an attempt to disperse CNT in polymer matrix such as in-situ polymerization, sonication, chemical modification through nanotube, mechanical mixing, etc. [30]. Modification of CNT surface can lead to the construction of chemical bonds between the nanotube and polymer matrix and offers the most efficient solution for the formation of strong interface.

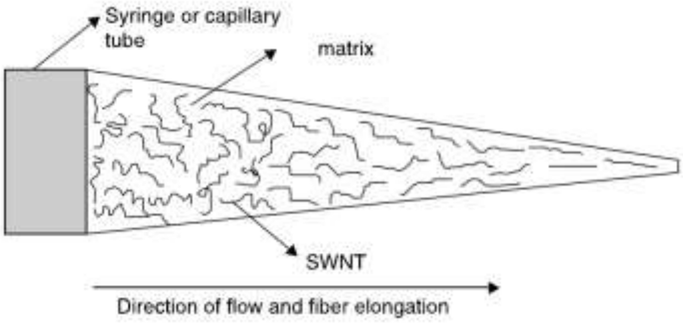

Figure 9. Schematic representation of CNT alignment during electrospinning composite nanofibers [30].

CHARACTERIZATION OF NANOFIBROUS MEMBRANE

Morphological study

In principle there are a large number of different characterization techniques that can be used to determine the properties of nanofibrous membranes. The morphology of nanofibrous membranes can be characterized by scanning electron microscopy (SEM). In SEM, the nanofibers sample, coated with a thin layer of a conductive material such as gold sputtered over its surface, is placed in a beam of high-energy electrons. Since nanofibrous membranes have porous structure, morphological properties include pore geometry and density (see Figure 10). As mentioned earlier, the final morphologies of the electrospun nanofibrous membranes can be affected by several characteristics of the initial solution such as solution concentration, viscosity, surface tension and conductivity of solution in addition to some electro-spinning processes (applied voltage, spinning distance, volume flow rate, and the strength of the applied electric field) and environmental conditions (temperature and humidity).

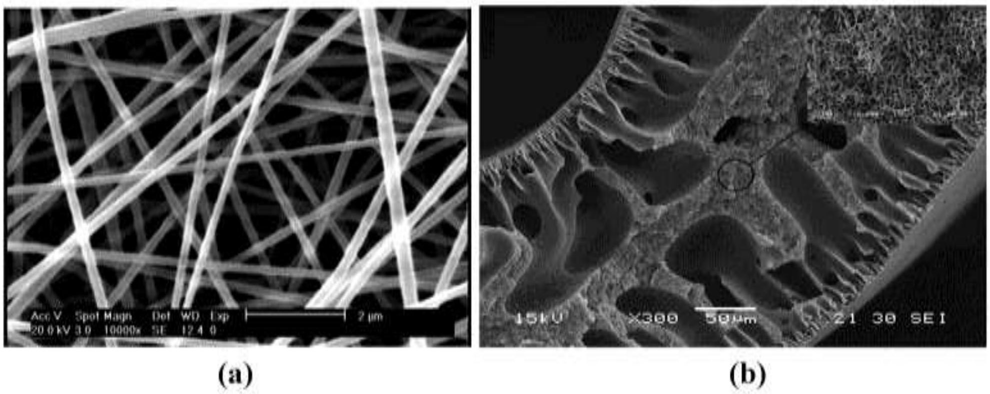

Figure 10. SEM micrograph of (a) electrospun nanofibrous membrane and (b) wet-spun composite hollow fiber membrane (cross-section view) [40].

Membrane performance study

The permeation flux, rejection, membrane porosity, and permeability are used to evaluate the membrane efficiency. The permeation flux (J) and rejection (R) of the membranes can be calculated from the following equations [40]:

$$J(l/m^2.h) = \frac{Q}{At} \tag{1}$$

$$R(\%) = \frac{C_f - C_p}{C_f} \times 100 \tag{2}$$

where J is the permeation flux of membrane for pure water; Q is the volume of the permeated solution (l); A is the effective area of the membrane (m^2); t is the permeation time (h); R is the solute rejection (%); C_p and C_f are the permeate and feed concentration (wt.%), respectively. The membrane porosity (ε) is defined as the volume of the pores divided by total volume of the porous membrane. It was usually determined by gravimetric method, by the weight of liquid contained in the membrane pores [40].

$$\varepsilon(\%) = \frac{(w_1 - w_2)}{\rho V} \times 100 \tag{3}$$

where ε is the membrane porosity (%); w_1 is the weight of the wet membrane (g); w_2 is the weight of the dry membrane (g); ρ is the solution density (g/cm) and V is the efficient volume of membrane samples (cm^3). Moreover, the membrane permeability (L_p) could be expressed by the following equation:

$$L_p(l/m^2.h.bar) = \frac{J}{\Delta P} \tag{4}$$

where L_p is the membrane permeability ($l/m^2.h.bar$) and ΔP is the effective pressure (bar).

Molecular weight cut-off (MWCO) measurement

The molecular weight cut off or MWCO is a specification commonly used to describe the retention capabilities of a membrane. This parameter is defined as the lower limit of a solute molecular weight e.g. poly(ethylene glycol) or dextran for which the rejection is greater than 90%. The MWCO specification is most commonly used to characterize ultrafiltration and nanofiltration membranes. As the MWCO decreases the mean pore diameter for most ultrafiltration membranes has been found to decrease. It should be mentioned that membrane surface characteristics e.g. surface porosity and pore size distribution may influence the apparent size of particles retained [41].

Decolorization assay via UV-Vis spectroscopy

For the measurement of absorption in UV-Vis region, beam spectrophotometers are most commonly used. Beer-Lambert law is then applied to determine quantitative concentration of an absorbing species in given solution.

$$A = Log(\frac{I_0}{I}) = \varepsilon \times b \times c \tag{5}$$

where A is the measured absorbance; I_0 is the intensity of the incident light at a given wavelength; I is the transmitted intensity; b is the path length through the sample (cm); c is the concentration of the absorbing species (mol/l) and ε is a constant known as the molar extinction coefficient (mol/l.cm) [42].

The percentage of decolorization could be calculated by using the formula as follows [43]:

$$\text{Decolorization}(\%) = \frac{OD_i - OD_f}{OD_i} \times 100 \tag{6}$$

where OD_i is the initial absorbance of dye (mg/l) and OD_f is the final absorbance of dye concentration (mg/l) at different time intervals.

CONCLUSION

Based on the results obtained in the percent study, we reached the following conclusions:

1. Nanofibrous membranes should have the following characteristics: high porosity, comparable mechanical and chemical properties, good flexibility, and good separability.
2. By modification of electrospinning process, it is possible to get several different types of nanofibrous membrane, such as porous, bicomponent, hollow, and composite nanofibers.
3. The use of porous nanostructured materials, such as CNTs, in composite nanofibrous membrane leads to improved absorption and mechanical properties.
4. The main parameters to be used to characterize the efficiency of nanofibrous membranes are permeation flux, rejection, membrane porosity, permeability, molecular weight cut off, and decolorization.

REFERENCES

1. Vandevivere P.C., Bianchi R., Verstraete W., 1998. Treatment and reuse of wastewater from the textile wet-processing industry: review of emerging technologies, *J. Chem. Technol. Biot.*, 72, 289-302.
2. Robinson T., McMullan G., Marchant R., Nigam P., 2001. Remediation of dyes in textile effluent: a critical review on current treatment technologies with a proposed alternative, *Bioresource. Technol.*, 77, 247-255.
3. Banat I.M., Nigam P., Singh D., Marchant R., 1996. Microbial decolourization of textile-dye containing effluents: a review, *Bioresource. Technol.*, 58, 217–27.
4. Slokar Y.M., Le Marechal A. M., 1998. Methods of decoloration of textile wastewaters, *Dyes. Pigments.*, 37, 335–356.
5. Dele´e W., ONeill C., Hawkes F.R., Pinheiro H.M., 1998. Anaerobic

treatment of textile effluents: a review, *J. Chem. Technol. Biot.*, 73, 323–335.

6. Cooper P., 1993. Removing color from dyehouse waste waters: a critical review of technology available, *J. Soc. Dyers. Colorists.*, 109, 97–100.
7. Crini G., Robert C., Gimbert F., Martel B., Adam O., De Giorgi F., 2008. The removal of Basic Blue 3 from aqueous solutions by chitosan based adsorbent: batch studies, *J. Hazard. Mater.*, 153, 96–106.
8. Dutta, P.K., Bhavani, K.D., Sharma, N.; 2001. Adsorption for dyehouse effluent by low cost adsorbent (chitosan), *Asian. Text. J.*, 10, 57–63.
9. Xu Y., Lebrun R.E., 1999. Treatment of textile dye plant effluent by nanofiltration membrane, *Sep. Sci. Technol.*, 34, 2501–2519.
10. Bechtold T., Burtscher E., Turcanu A., 2001. Cathodic decolorisation of textile wastewater containing reactive dyes using multi-cathode electrolyser, *J. Chem. Technol. Biot.*, 76, 303–311.
11. Papic S., Koprivanac N., Bozic A.L., Metes A., 2004. Removal some reactive dyes from synthetic wastewater by combined Al (III) coagulation/carbon adsorption process, *Dyes. Pigments.*, 62, 291–298.
12. Akhtar N., Iqbal J., Iqbal M., 2004. Enhancement of Lead(II) biosorption by microalgal biomass immobilized onto Loofa (Luffa cylindrica) sponge, *Eng. Life. Sci.*, 4, 171–178.
13. Kahraman S., Asma D., Erdemoglu S., Yesilada O., 2005. Biosorption of Copper(II) by live and dried biomass of the white rot fungi Phanerochaete chrysosporium and Funalia trogii, *Eng. Life. Sci.*, 5, 72–77.
14. Marrot B., Roche N., 2002. Wastewater treatment and reuse in textile industries, a review, *Res. Adv. In Water Res.*, 3, 41-53.
15. Aptel P., Buckley C.A., 1996. Categories of membrane operations. in ‘water treatment: membrane process’ (eds.: Mallevialle J., Odendaal P.E. and Winsner M.R.) McGraw-Hill, New York.
16. Ondarçuhu T., Joachim C., 1998. Drawing a single nanofibre over hundreds of microns, *Europhys. Lett.*, 42, 215–220.
17. Feng L., Li S., Li Y., Li H., Zhang L., Zhai J., Song Y., Liu B., Jiang L., Zhu D., 2002. Super-hydrophobic surfaces: from natural to artificial, *Adv. Mater.*, 14, 1221–1223.
18. Ma P.X., Zhang R., 1999. Synthetic nano-scale fibrous extracellular matrix, *J. Biomed. Mater. Res.*, 46, 60–72.
19. Liu G., Ding J., Qiao L., Guo A., Dymov B.P., Gleeson J.T., Hashimoto T.K., Saijo K., 1999. Polystyrene-block-poly(2-cinnamoyl ethyl methacrylate) nanofibers preparation, characterization, and liquid crystalline properties. *Chem-A Eur. J.*, 5, 2740–2749.
20. Doshi J., Reneker D.H., 1995. Electrospinning process and applications of electrospun fibers, *J. Electrostat.*, 35, 151–160.
21. Shams Nateri A., Hasanzadeh M., 2009. Using fuzzy-logic and neural network techniques to evaluating polyacrylonitrile nanofiber diameter. *J. Comput. Theor. Nanosci.*, 6, 1542-1545.
22. Haghi A.K., Akbari M., 2007. Trends in electrospinning of natural nanofibers. *Phys. Status. Solidi. A.*, 204, 1830-1834.

23. Ziabari M., Mottaghitalab V., Haghi A.K., 2009. A novel approach for analysis of processing parameters in electrospinning of nanofibers. in ‘Nanofibers: fabrication, performance, and applications’ (ed. Chang W.N.) Nova Science Publishers, New York.
24. Hadavi Moghadam B., Hasanzadeh M., Haghi A.K. 2013. On the contact angle of electrospun polyacrylonitrile nanofiber mat. *Bulg. Chem. Commun.*, 45, 169-177.
25. Hasanzadeh M., Hadavi Moghadam B., Moghadam Abatari M.H., Haghi A.K., 2013. On the production optimization of polyacrylonitrile electrospun nanofiber. *Bulg. Chem.Commun.*, 45, 178-190.
26. Hadavi Moghadam B., Hasanzadeh M., 2013. Predicting contact angle of electrospun polyacrylonitrile nanofiber mat by artificial neural networks and statistical techniques. *Adv. Polym. Tech.*, doi: 10.1002/adv.21365,
27. Rabbi R., Nasouri K., Bahrambeygi H., Shoushtari A.M., Babaei M.R., 2012. RSM and ANN approaches for modeling and optimizing of electrospun polyurethane nanofibers morphology. *Fiber. Polym.*, 13, 1007-1014.
28. Sabetzadeh N., Bahrambeygi H., Rabbi A., Nasouri K., 2012. Thermal conductivity of polyacrylonitrile nanofiber web in various nanofiber diameters and surface densities. *Micro. Nano. Lett.*, 7, 662-666.
29. Rošic R., Pelipenko J., Kristl J., Kocbek P., Baumgartner S., 2012. Properties, Engineering and Applications of PolymericNanofibers: Current Research and Future Advances. *Chem. Biochem. Eng. Q.*, 26, 417–425.
30. Andrady A.L., 2008. Science and technology of polymer nanofibers. Wiley, USA.
31. Brown P.J., Stevens K., 2007. Nanofibers and nanotechnology in textiles. Woodhead, England.
32. Sun Z., Zussman E., Yarin A.L., Wendorff J.H., Greiner A., 2003. Compound core-shell polymer nanofibers by co-electrospinning, *Adv. Mater.*, 15, 1929-1932.
33. Ramakrishna S., Fujihara K., Teo W.E., Lim T.C., Ma Z., 2005. An introduction to electrospinning and nanofibers. World scientific, Singapore.
34. Zussman E., Yarin A.L., Bazilevsky A.V., Avrahami R., Feldman M., 2006. Electrospun polyacrylonitrile/poly(methyl methacrylate)-derived turbostratic carbon micro-/nanotubes, *Adv. Mater.*, 18, 348-353.
35. Nasouri K., Shoushtari A.M., Kaflou A., Bahrambeygi H., Rabbi A., 2012. Single-wall carbon nanotubes dispersion behavior and its effects on the morphological and mechanical properties of the electrospun nanofibers, *Polym. Composite.*, 33, 1951-1959.
36. Yang S.Y., Taha-Tijerina J., Serrato-Diaz V., Hernandez K., Lozano K., 2007. Dynamic mechanical and thermal analysis of aligned vapor grown carbon nanofiber reinforced polyethylene. *Composites B*, 38, 228–235.
37. Bahrambeygi H., Sabetzadeh N., Rabbi A., Nasouri K., Shoushtari A.M., Babaei M.R., 2013. Nanofibers (PU and PAN) and nanoparticles (Nanoclay and MWNTs) simultaneous effects on

polyurethane foam sound absorption. *J. Polym. Res.*, 20, 1-10.

38. Al-Saleh M.H., Sundararaj U., 2011. Review of the mechanical properties of carbon nanofiber/polymer composites. *Composites A*, 42, 2126-2142.
39. Moridi Z., Mottaghitalab V., Haghi A.K., 2011. A Detailed Review of Recent Progress in Carbon Nanotube/Chitosan Nanocomposites. *Cellulose Chem Technol*, 45, 549-563.
40. Han L.F., Xu Z.L., Yu L.Y., Wei Y.M., Cao Y., 2010. Performance of PVDF/multi-nanoparticles composite hollow fibre ultrafiltration membranes, *Iran. Polym. J.*, 19, 553-565.
41. Boerlage S. F. E., 2001. Scaling and particulate fouling in membrane filtration systems. Swets & Zeitlinger Publisher, Lisse.
42. McDonald R., 1997. Colour physics for industry. Society of Dyers and Colourists, London.
43. Dorthy C.A.M., Sivaraj R., Venckatesh R., 2012. Decolorization of reactive violet – 2RL dye by aspergillus flavus and aspergillus fumigatus from textile sludge, *Int. Res. J. Environ. Sci.*, 1, 8-12.